Optimization
Iranian Journal of Optimization
Volume 14, Issue 2, 2022, 135-156
Research Paper

Online version is available on: www.ijo.rasht.iau.ir

Islamic Azad University
Rasht Branch
ISSN: 2588-5723
E-ISSN:2008-5427

An Artificial Neural Network Method to Predict the COVID-19 Cases in Iran

Meisam Shamsi[1], Reza Babazadeh[1*] and Mohsen Varmazyar[2]

[1]Faculty of Engineering, Urmia University, Urmia, West Azerbaijan Province, Iran

[2]Department of Industrial Engineering, Sharif University of Technology, Tehran, Iran

Revise Date 29 July 2022
Accept Date: 16 August 2022

Abstract

The sudden emergence of a Coronavirus and its rapid spread due to the globalization factors, especially the airline network, provoked the reaction of countries. Governments attempt to use all available means, including prediction methods, to control the spread of the Coronavirus. In this article, we have developed various models based on artificial neural networks, including multi-layer perceptron, radial basis function, and adaptive-network-based fuzzy inference system with different learning algorithms, transfer functions, membership functions, hidden layers, hidden neurons, and kernels. We have identified five factors influencing the Coronavirus outbreak based on the Pearson correlation coefficient approach. These factors are gasoline consumption, internet pressure, number of wedding ceremonies, online transactions, and mask consumption. The accuracy of the developed models is identified by calculating three types of statistical errors, including root mean square error, mean absolute error, and mean absolute percentage error. The results show that the radial basis function model predicts the number of Covid-19 cases for the one month (mid-term) with an accuracy of over 97%. This study provides an efficient approach to predict the number of COVID-19 cases which help policymakers to make strategic decisions, including closing borders, designing supply chains for medical and health equipment, and enacting new laws.

Keywords:
Covid-19
Predict
Artificial neural network
Radial basis function
Adaptive-network-based fuzzy inference system

***Correspondence E-mail**: r.babazadeh@urmia.ac.ir

INTRODUCTION

On January 30, 2020, the World Health Organization (WHO) announced a new coronavirus and declared a public health emergency of international concern. On February 11, 2020, the WHO officially named the virus "COVID-19". The outbreak of the COVID-19 virus in Wuhan, China, in January 2020, and its spread worldwide in less than two months, has worried all countries and caused extensive damages (Alakus & Turkoglu, 2020).

The COVID-19 virus has spread to almost every country in the world, affecting all nations of the world, infecting millions of people, killing hundreds of thousands, and almost disrupting the world economy, and has challenged countries and nations politically and socially (Guhathakurata et al., 2022). COVID-19 is a complex issue, and assuredly has pervasive consequences. COVID-19 management and control require accurate information and knowledge of its behavior. The COVID-19 pandemic has created a wave of change in social, cultural, and economic dimensions, So this phenomenon has changed from a medical phenomenon to a social, economic, and political phenomenon. Some areas affected by the COVID-19 pandemic include economy, society, and politics. In the following, the effect of COVID-19 spread in these areas are studied.

- *Economy*

The COVID-19 epidemic does not only affect human health. The first and the most important effect of this disease is felt in world economics. The countries' economics seem to be in turmoil because it is unclear how far the disease will go? When can it be controlled? What damage will it do to human health? Moreover, will a similar pandemic occur again? From an economic perspective, the damage caused by the COVID-19 virus epidemic is mainly due to declining demand; This means that there is no consumer to buy goods and services in the global economy (Barua, 2021). Decreasing demand leads to lower corporate revenues; hence companies are forced to reduce their workforce and these unemployed workers are unable to buy goods and services, and again downturn in the economy. The COVID-19 epidemic has reversed China's economic growth and disrupted production in this country, and the European economy has stalled as the disease spread to Italy, France, Germany, and Spain. This trend's continuity may lead to a global economic crisis and could drown countries with fragile economies in this crisis (Jackson, 2021).

- *Society*

Implementing policies such as social distancing and the closure of public places such as parks, cafes, shrines, schools, universities, clubs, etc., and preventing people from attending these places will have inevitable social consequences. The closure of schools and universities will also deprive millions of children, adolescents, and young people of educational and social activities for a long time, which may not be easily compensated later. On the other hand, the continuity of forced or voluntary self-isolation will have devastating effects on pre-vulnerable groups such as people with depression and anxiety.

- *Politics*

COVID-19 is one of the most influential phenomena that has changed the structure of international political relations. The spread of the virus and the global response to it have taken on many dimensions. COVID-19 is a tremendous global test to show the effectiveness of globalization. The sudden emergence of COVID-19 in more than 200 countries in less than 100 days, regardless of geographical and political boundaries, has severely impacted globalization's dimensions (Bickley et al., 2021). International affairs experts believe that the decades-old order

of the global structure will change during this period. In the post-COVID-19 era, we will probably see the importance of borders again and the intensification of national controls, eventually weakening globalization.

Furthermore, the legitimacy of governments depends on the control and management of the COVID-19 pandemic. People are asking questions such as: does the government care about the health of its citizens? And does the government have the ability to ensure the health of its citizens against COVID-19? Governments that fail to control and manage the COVID-19 pandemic will lose their popularity and legitimacy and will be replaced by a rival faction in the next election.

According to the mentioned reasons, the COVID-19 outbreak can cause irreparable damage to a country; hence it is essential to use all available tools and methods to control and manage the COVID-19 outbreak to reduce its destructive effects. One of the fundamental approaches to control critical situations is to use forecasting techniques to predict the number of COVID-19 cases. These predictions are not used only to know the future situation; the main purpose is to control the existing conditions to achieve the desired conditions and help policymakers to control and manage the prevalence of COVID-19 more effectively. Decisions making about supplying medicines and emergency products, hospitals' variable capacity, closing government and non-government centers, setting up field hospitals, and enacting mandatory home quarantine legislation depend on the proper prediction of the COVID-19 cases.

In this study, we provide three approaches to predict the number of COVID-19 cases. These approaches include Multi-Layer Perceptron Artificial Neural Network (MLP-ANN), Radial Basis Function Artificial Neural Network (RBF-ANN), and Adaptive-Network-Based Fuzzy Inference System (ANFIS). The main objectives of this research can be summarized as follows:

- To provide a prediction study for the number of COVID-19 cases with machine learning application models for Iran,
- To ensure the accuracy of the innovative prediction model.

The rest of the paper is organized as follows. The related work with artificial neural networks (ANN), Radial Basis Function (RBF), and ANFIS are presented in the next section. The MLP-ANN, RBF-ANN, and ANFIS methods are described in the third section. In the fourth section, the influential components of the COVID-19 outbreak are introduced. Case study, data acquisition and correlation coefficient calculations are also presented in this section. The obtained results are analyzed in the fifth section. The last section provides a general conclusion.

RELATED WORK

Artificial neural networks (ANN) should be considered as a vast field of the intersection of sciences such as computer science, engineering, biology, and communication. ANN can be used to extract patterns from complex data by inferring meanings that are complex to the human brain (Kong et al., 1999). ANNs cannot be programmed to perform a specific task. The advantage of a neural network is that it discovers how to solve the problem by itself (Mitchell & Mitchell, 1997). The network should be trained with several examples so that it finds the relationship between the variables. After the training phase, the network can predict the desired values for an output parameter based on a new data set (Barto, 1984). In recent years, a variety of prediction studies have been conducted using ANN models. Sadek et al. Sadek et al., (2019) have developed an ANN model that helps doctors to diagnose Parkinson's Disease in its early stages. Al-Shawwa & Abu-Naser (2019) presented an ANN model that was able to predict the weight of

newborns with 100% accuracy. Acheampong & Boateng (2019) predicted carbon dioxide emissions in the USA, China, India, Brazil, and Australia via the ANN approach. The achieved results showed insignificant errors between actual values and predicted values.

Radial Basis Function (RBF) approach is one of the prediction methods using artificial neural network structure. RBF networks are widely used to estimate nonparametric multidimensional functions using a limited set of data (Hartman et al., 1990). RBFs are inspired by statistical clustering techniques, and their main capability is to find patterns between dependent and independent variables in nonlinear space. Various applications for RBF are presented in the articles. Li et al., (2017) modeled the irregular flow of Beijing subway passengers by proposing a multiscale radial basis function. The developed model was able to estimate the volume of subway passengers on specific days. Kouser et al., (2018) provided a two-step framework for heart disease prediction. An ANN model was developed for the first stage that enabled doctors to predict heart disease in a patient. In the second stage, a neural network based on RBF was developed to prescribe the necessary medicines to the patient. Tatar et al., (2016) showed that the RBF neural network has the ability to predict surfactant retention in petroleum industries, accurately.

ANFIS is a hybrid method consisting of a fuzzy system and a neural network. ANFIS utilizes the training power of neural networks and fuzzy logic, which is based on if-then rules to analyze very complex processes. Today, fuzzy systems based on the adaptive neural network are widely used for modeling and prediction purposes as an efficient tool (Nayak et al., 2004). Mohandes et al., (2011) implemented the ANFIS method to estimate wind speeds at altitudes above 100 meters to determine the best locations for wind farms. Emamgholizadeh et al., (2014) used both ANN and ANFIS models to predict the groundwater level of Batam plain in Iran. The results showed that both methods are capable of accurate prediction. Mirrashid (2014) developed an ANFIS model with a fuzzy C-means algorithm to predict earthquakes with a magnitude above 5.5. The obtained results proved the high accuracy of the developed model.

METHODOLOGY

This study was designed to apply three well-known ANN modeling approaches, MLP-ANN, RBF-ANN, and ANFIS, to predict the number of COVID-19 cases. The proposed approaches are explained in the following section. Multi-Layer Perceptron Artificial Neural Network (MLP-ANN) The general structure of ANN is inspired by the human biological neural network. In this study, a feed-forward MLP-ANN is developed due to its ability to produce high-quality results. The overall structure of the MLP-ANN is presented in Fig. 1. An MLP-ANN consists of one input layer, one or multiple hidden layers, and one output layer. In this type of network, the input values are converted to output values passing through all layers.

Each layer consists of neurons, which are the processing units of the MLP-ANN. Each neuron receives data as input values from its previous layer. The number of neurons in the input layer equals to the number of network inputs. Similarly, the number of neurons in the output layer equals to the number of network outputs. The number of hidden layers and neurons within them are determined based on the trial and error method. The overall layout of a single artificial neuron is shown in Fig. 2. The input values of each neuron are multiplied by their corresponding weights. Then the total weighted input values are summed up with another value called "bias." The value gained from the previous step is fed to a nonlinear function known as a transfer function to generate neuron's output value

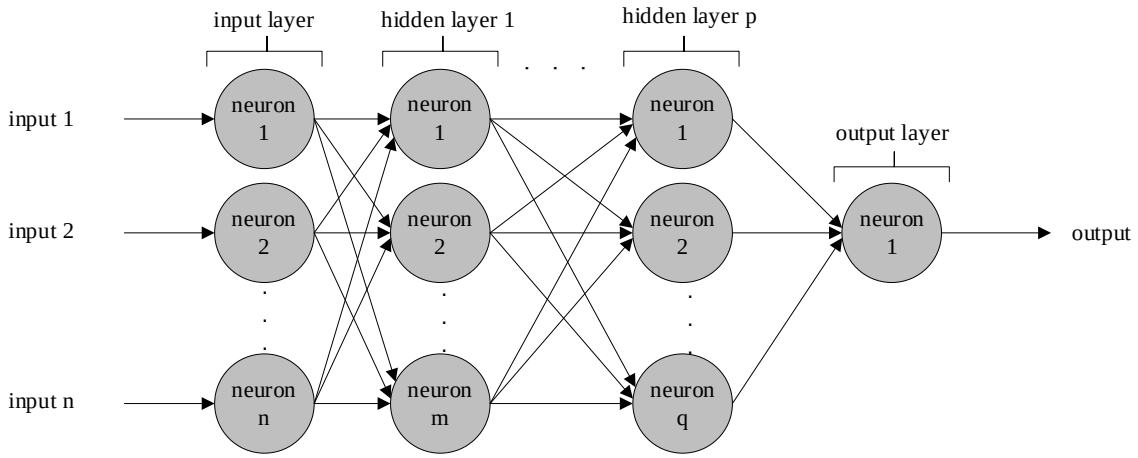

Fig. 1. MLP artificial neural network structure

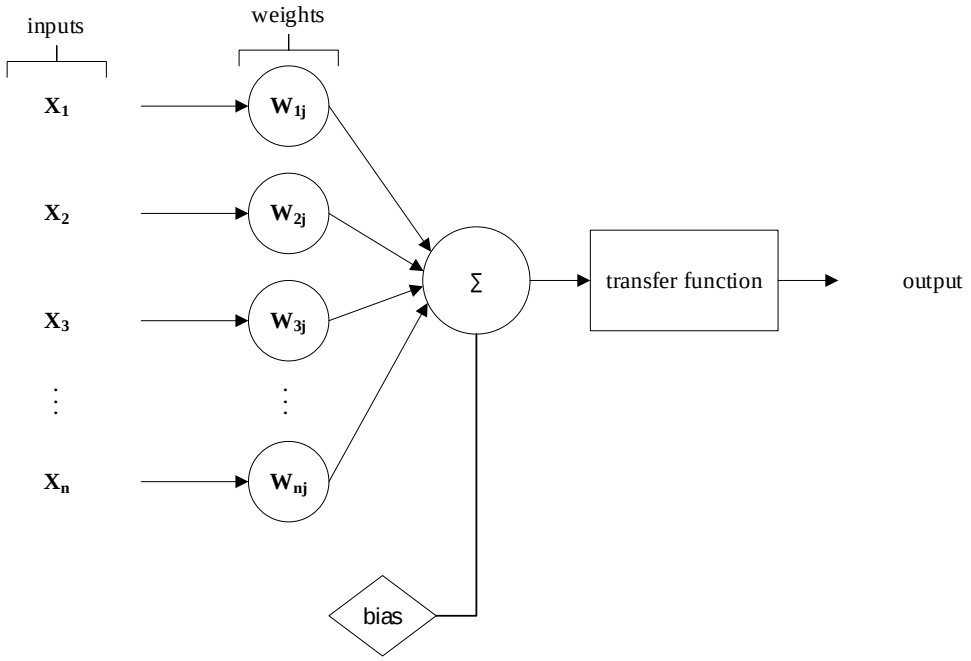

Fig. 2. Single artificial neuron layout

MLP-ANN can learn from examples to produce the desired output. The learning process is implemented by comparing the model output values with actual output values, known as target values. There are two types of learning algorithms: supervised and unsupervised. The propagation algorithm with a Levenberg-Marquardt training function is one of the popular supervised learning algorithms that has proven its efficiency in various researches. In this algorithm, random values are assigned to weights and biases before the learning process begins. In the first step, the model's input values are converted to model output values through transfer function within each layer's neurons. Then the difference between obtained output values and the target

values, called an error signal, is calculated. The error signals are then propagated to the network neurons to determine the new values of weights and biases. This process will continue until the model outputs are as close as possible to the target values. The most commonly used transfer functions for back-propagation are as follows:

PURELIN transfer function, which is a linear function, is expressed as:

$$a = purelin(n) = \sum_{i=1}^{N} X_i \times W_{ip} + b_p \quad (1)$$

TANSIG transfer function, which is a hyperbolic tangent sigmoid function is defined as:

$$a = tansig(n) = \frac{2}{1 + \exp(n)} - 1 \quad (2)$$

LOGSIG transfer function, which is a logistic function, is expressed as:

$$a = logsig(n) = \frac{1}{1 + \exp(-n)} \quad (3)$$

Where n is the number of inputs, X_i is the input value of neuron i, W_{ip} is the weight of neuron i in hidden layer p, and b_p is the bias value of hidden layer p.

Radial Basis Function Artificial Neural Network (RBF-ANN)

RBF is another type of ANN which have a faster training algorithm than MLP-ANN. The main advantage of these networks is that they do not find optimal local values (Chen et al., 2019). RBF-ANNs consist of three layers: The input layer, which holds input data. The hidden layer in which the network kernels are located. An output layer, which calculates the output value of the network. The general structure of the RBF-ANN and its kernels is illustrated in Fig. 3 and Fig. 4, respectively.

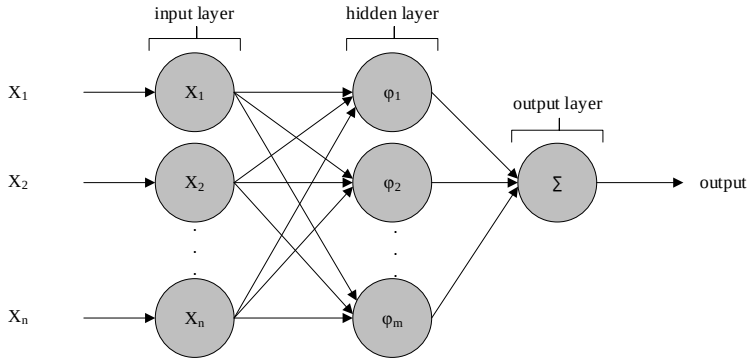

Fig. 3. RBF artificial neural network structure

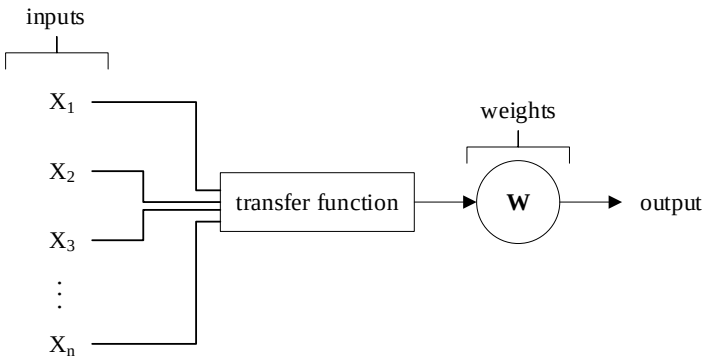

Fig. 4. RBF kernel layout

The input layer data is passed to the hidden layer's kernels without any specific modification. The received data in the kernels are passed through the transfer function within each kernel; thus, the kernels' output is calculated. The output of each kernel is then multiplied by its corresponding weight. The network's output value is calculated by the summation of all weighted values achieved from the previous step plus another value known as 'bias.' The kernels and output layer calculations are shown in equations (4) and (5), respectively.

$$\hat{y}_m = W_m \times \varphi_m(x) \quad (4)$$

$$y = \sum_{i=1}^{m} W_m \times \varphi_m(x) + B \quad (5)$$

Where $\hat{y}_m$ is the output of *mth kernel*, x is the network's input values, W_m is the weight if *mth* kernel, φ_m is the transfer function in *mth* kernel, y is the network's output, and B is the value related to bias.

In the current study, the Gaussian function is considered as the transfer function for the kernels:

$$\varphi_m(x) = exp\left(-\frac{\|X - c_m\|}{\theta_m^2}\right) \quad (6)$$

Where c_m is the center, and θ_m is the spread of the *mth* kernel. The RBF is optimal when the network's outputs are as close as possible to actual output values known as target values. The accuracy of RBF depends on determining proper values for the centers, weights, spread, and the number of kernels in the hidden layer. The number of kernels and the spread value are specified by the trial and error method. The optimum values for the centers and weights are calculated during the training process. In this study, Orthogonal Least Square (OLS) technique is applied for the training process. OLS method uses the gram-Schmidt algorithm to find the optimal centers and uses the adaptive gradient descent algorithm to update the weight values.

Adaptive Neuro-fuzzy Inference System (ANFIS)

The ANFIS network provides an efficient prediction tool by combining the capabilities of fuzzy logic and ANN learning ability. ANFIS's inference system corresponds to a set of fuzzy if-then rules that have learning capability to estimate nonlinear functions. In the current study, the fuzzy system of the ANFIS network is based on the Sugeno model. Fig. 5 shows the ANFIS structure.

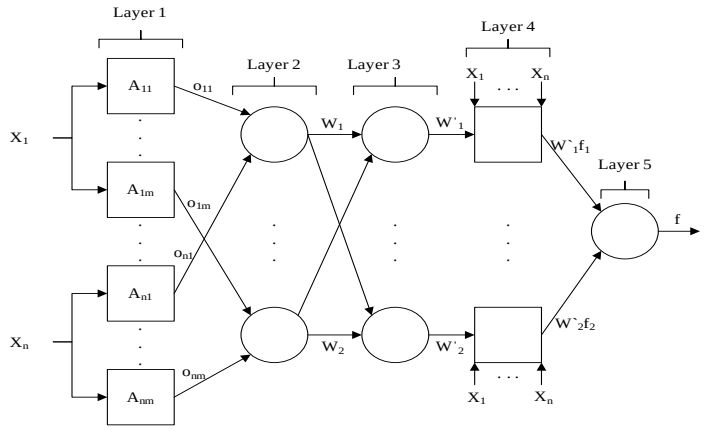

Fig. 5. ANFIS artificial neural network structure

The overall structure of the ANFIS network is similar to MLP-ANN. The layer one act as the input layer, layer two and three act as the hidden layers, and layer four and five, act as the output layer in MLP-ANN. Each layer in ANFIS has its own function and specific task. According to *Fig.* **5**, the architecture of ANFIS is composed of five layers: fuzzification layer, rule layer, normalization layer, defuzzification layer, and output layer, respectively.

The first layer takes the input values and determines the membership functions belonging to them. During this step, the standard inputs (crisp inputs) are transformed into fuzzy inputs. Consider two inputs and one output for the ANFIS network shown in *Fig.* **5**. The fuzzification process can be formulated as follow:

$$o_{1i} = \mu_{A1i}(x_1) \quad i = 1,2 \tag{7}$$

$$o_{2i} = \mu_{A2i}(x_2) \quad i = 1,2 \tag{8}$$

Where x_1 and x_2 are the input values, $A1i$ and $A2i$ are the fuzzy variables corresponding to each input variable, o_{1i} and o_{2i} are the membership function of fuzzy set $A1i$ and $A2i$, respectively.

The second layer is responsible for generating the firing strengths for the rules which can be calculated with equation (9):

$$w_i = \mu_{A1i}(x_1)\mu_{A2i}(x_2) \quad i = 1,2 \tag{9}$$

The role of the third layer is to normalize the computed firing strengths. The fuzzy inference system proposed by Takagi and Sugeno (Takagi & Sugeno, 1983) is used for the calculation:

$$w'_i = \frac{w_i}{w_1+w_2} \quad i = 1,2 \tag{10}$$

The fourth layer takes the normalized values achieved from the previous step and also the consequence parameter set which are p_i, q_i, r_i as the input parameters. The output of each rule is a linear combination of input variables:

$$w'_i f_i = w'_i(p_i x_1 + q_i x_2 + r_i) \quad i = 1,2 \tag{11}$$

p_i, q_i, r_i are parameter sets, which can be identified by the least square algorithm.

The fifth layer calculated the final output of all rules:

$$y = \sum_{i=1}^{2} w'_i f_i = \frac{\sum_{i=1}^{2} w_i f_i}{\sum_{i=1}^{2} w_i} \quad i = 1,2 \tag{12}$$

The ANFIS should be trained to determine the optimal values for the nonlinear parameters related to the fuzzy membership functions in the first layer and the linear parameters of the fourth layer so that the model can generate the desired outputs. The hybrid learning method is one of the most common algorithms for training the ANFIS network. In this algorithm, the Back-Propagation method is used to train the first layer, and the Least-Squares Estimator (LSE) approach is used to train the fourth layer (Jang & Sun, 1995).

$$RMSE = \sqrt{\frac{\sum_{i=1}^{n}(|T_i - P_i|)}{n}} \tag{13}$$

$$MAE = \frac{\sum_{i=1}^{n}(|T_i - P_i|)}{n} \tag{14}$$

$$MAPE = \frac{\sum_{i=1}^{n}\frac{(|T_i - P_i|)}{Ti}}{n} \times 100 \tag{15}$$

Where T_i is the target value, P_i is the predicted value, and n is the number of data. It should be noted that the target value is known and is also called the observed value.

CASE STUDY AND DATA ACQUISITION

The case study and data acquisition are presented in this section.

Case study

We consider the Iranian population for our case study. The data set used in this paper is taken from the Ministry of Health and Medical Education (Government of Iran). It should be noted that the data were collected for five months (March 1, 2020 - July 31, 2020). According to WHO, it takes an average of six days for COVID-19 symptoms to appear in an infected person. Therefore, the data collected for n^{th} day corresponds to the number of COVID-19 cases in the $(n + 8)^{th}$ day.

Data acquisition

The efficiency of artificial intelligence and, consequently, machine learning algorithms decreases as the number of input parameters increases (Abbas et al., 2019). Therefore, only the parameters that have the most significant impact on the forecast should be selected to make the model accurate. In this study, a range of factors influencing the prevalence of COVID-19 disease was examined. Finally, five significant factors were adopted based on the Pearson correlation coefficient (PCC) value.

$$\mathrm{PCC} = \frac{\mathrm{cov}(X, Y)}{\sigma_X \sigma_Y} \quad (16)$$

Where X is the input variable, Y is the output variable, COV is the covariance, σ_X is the standard deviation of X, and σ_Y is the standard deviation of Y.

Each of the selected input parameters is an aggregation of multiple factors affecting the output parameter. The purpose of this integration is to reduce the number of input parameters. The selected parameters are as follows:

- Gasoline consumption

According to the Iran Ministry of Health (https://behdasht.gov.ir) and the WHO, one of the leading reasons for the spread of COVID-19 is intercity and urban traveling. People go on urban trips mostly for going to work, shopping, and meeting relatives, using public transportation such as taxis and buses, which leads to a reduction in social distancing and increases the risk of COVID-19 infection. Daily gasoline consumption can indicate the amount of intercity and urban travels. The data for gasoline consumption is achieved from the Iran Ministry of Petroleum (https://www.mop.ir)

- Internet pressure

According to the KASPR Datahaus (https://kasprdata.com), the amount of internet pressure has increased rapidly during the COVID-19 outbreak due to home quarantine. Most people spend their spare time on the internet at home. The increase in internet pressure mainly stems from using video on demand (VOD) services, social media, online shopping, online video games, and online educational services during the COVID-19 outbreak. Therefore, high internet pressure indicates the observance of health protocols based on the "stay home" slogan. Staying home means social distancing, which slows down the COVID-19 outbreak. The data for internet pressure is obtained from the KASPR Datahaus website.

- Registered wedding ceremony

In July 2020, Iran witnessed a rapid growth in the number of COVID-19 cases. The Iranian Ministry of Health acknowledged that the main reason for this upward trend was wedding ceremonies. Many people gather in a closed space at wedding ceremonies, which is contrary to the social distancing policy and could lead to the spread of COVID-19. The data for the number of wedding ceremonies is acquired from Iran National Organization for Civil Registration (https://www.sabteahval.ir).

- Online Transactions

The COVID-19 outbreak impacts on consumers' payment behavior. The social distancing policy encourages people to use digital methods and do online shopping to buy their needs instead of shopping in-person. This change in consumers' behavior reduces the use of cash and social interactions, which leads to a deceleration in the Covid-19 outbreak. The data for online transactions are gained from the Central Bank of Iran (https://www.cbi.ir).

- Mask consumption

The use of masks is one of the most important measures to prevent and control infectious diseases like COVID-19. Healthy people use masks to protect themselves from being infected, and infected people use masks to prevent transmission. The data for mask consumption as achieved from Iran Ministry of Industry, Mine, and Trade (https://www.mimt.gov.ir).

A summary of the collected data is presented in Table **1**. The complete data set is also presented in the appendix.

Table 1: Summary of collected data for input parameters

Input parameters	Range	Mean	Std. Deviation
Gasoline Consumption (Liter)	24-142	87	26.284
Internet Pressure (IP)	1.372-17.186	8.749	3.276
Wedding Ceremony (number)	988-8621	5015	1731.443
Online Transaction (Thousand Billion IRR*)	0.443-3.338	1.649	0.716
Mask Consumption (number)	379630-810366	603391	81660.416

* Iranian Rials

The Pearson correlation coefficient (PCC) value between the selected input parameters and the number of daily COVID-19 cases is presented in *Table 2*. The SPSS software is utilized for PCC calculation.

Table 2: Pearson correlation coefficient value for input parameters

	Gasoline Consumption	Internet Pressure	Mask Consumption	Online Transactions	Wedding Ceremony
PCC	0.981	-0.836	-0.8	-0.913	0.997

The calculated PCC values indicate a high correlation between input parameters and the output variable. Gasoline consumption and the number of wedding ceremonies have positive values, which means they have a direct relation with the output variable. Internet pressure, mask consumption, and online transactions have negative values, which means they have an inverse relation with the output value. Hence, an increase in the value of gasoline consumption and wedding ceremony numbers has a positive effect on the output variable, and an increase in the value of internet pressure, mask consumption, and online transaction have a negative effect on the output variable. This analysis shows that the acquired data are reliable and therefore the achieved results could be used, confidently.

RESULTS

The results of three approaches, MLP-ANN, RBF-ANN, and MLP-ANN based on collected data are presented in this section.

Multi-Layer Perceptron Artificial Neural Network (MLP-ANN)

A MLP-ANN includes two major steps: training and testing the model. The collected data sets (153

data) are divided into three groups: training data set (130 data), validation data set (15 data), and test data set (8 data). The training data set is used to train the model. The validation data set is used to determine whether the model is being trained enough for prediction or not? The test data is used to evaluate model performance. It should be noted that the data for each group of sets is selected randomly in each run. The MLP-ANN performance depends on determining three parameters: the number of hidden layers, the number of neurons in each hidden layer, and the type of transfer functions. Various numbers of hidden layers and hidden neurons, as well as three types of transfer functions, were used to develop MLP-ANN models. The best network is the one with the lowest MAE, RMSE, and MAPE value. More than 50 MLP-ANN models were developed to investigate the optimal structure for prediction. We have named the models according to their structure for a more straightforward comparison. "ML_1" models have two hidden layers with TANSIG transfer function in both hidden layers. "ML_2" models are composed of two hidden layers with TANSIG transfer function in the first hidden layer and LOGSIG transfer function in the second hidden layer. "ML_3" models consist of three hidden layers with the TANSIG transfer function. "ML_4" models are like "ML_3" except that the LOGSIG transfer function is used in the third hidden layer. All models have PURELIN transfer function in the output layer. Table 3 shows the best structure for each model. Indeed, model 1 represents the best structure among ML_1 models. A graphical presentation of the actual and predicted values by the MLP-ANN models for eight days is presented in Fig. 6 to Fig. 9.

Table 3: The best error values for different structures of the MLP-ANN models

Model	Network Topology	Error		
		MAE	RMSE	MAPE(%)
Model 1	[3-3] [TANSIG - TANSIG]	34.008	43.800	1.916
Model 2	[3-4] [TANSIG - LOGSIG]	32.035	37.908	1.377
Model 3	[4-3-6] [TANSIG - TANSIG - TANSIG]	22.142	28.379	1.199
Model 4	[4-3-6] [TANSIG - TANSIG - LOGSIG]	23.578	35.555	1.045

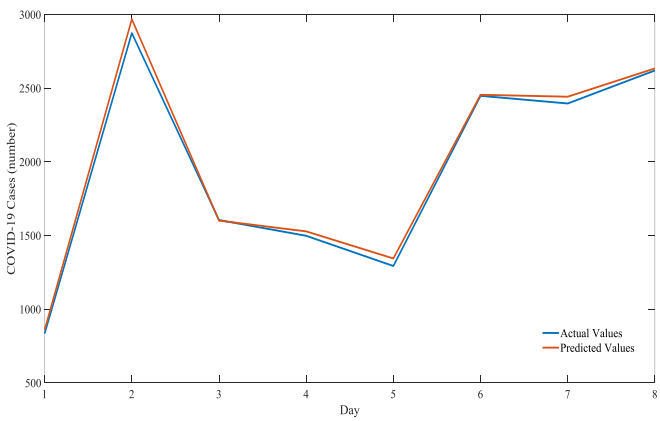

Fig. 6. Actual vs. predicted values for COVID-19 cases with Model 1 for eight days

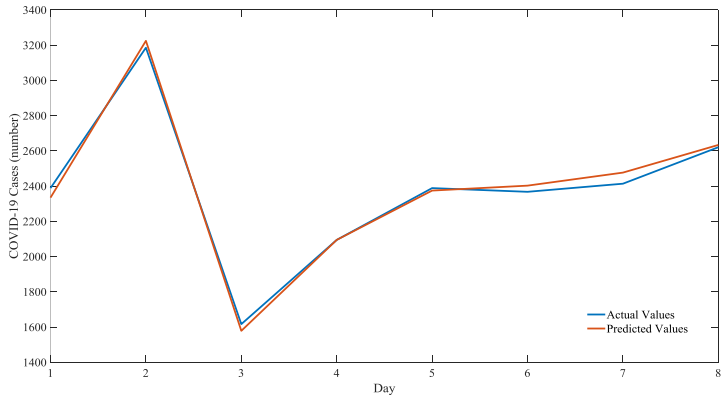

Fig. 7. Actual vs. predicted values for COVID-19 cases by Model 2 for eight days

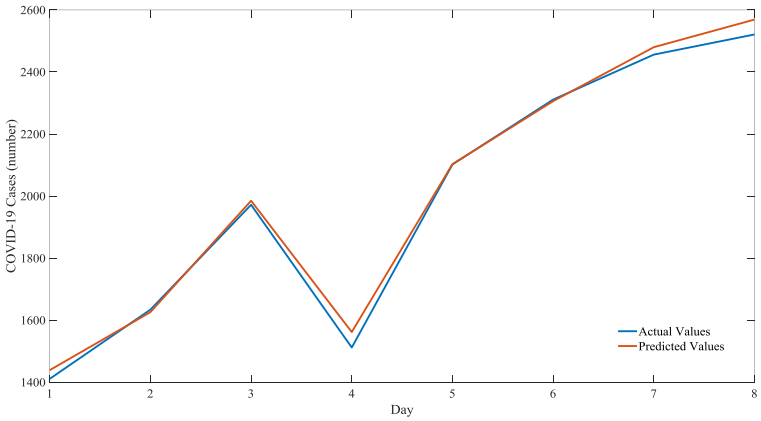

Fig. 8. Actual vs. predicted values for COVID-19 cases with Model 3 for eight days

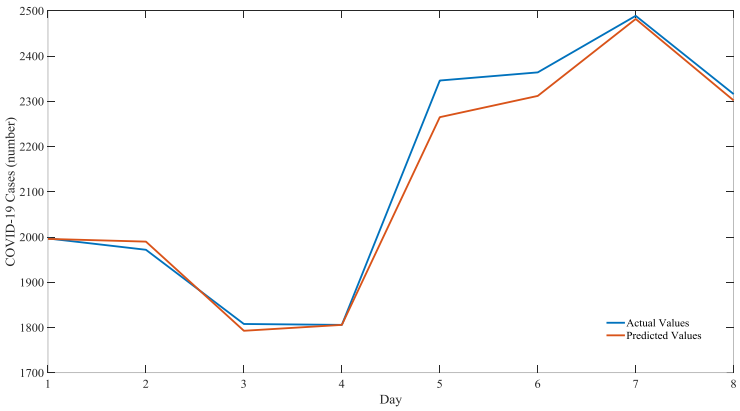

Fig. 9. Actual vs. predicted values for COVID-19 cases with Model 4 for eight days

The results showed that all developed networks with the structure of ML_1 models are all able to produce the desired output with a slight difference from each other (see figures 1 and 3). The achieved results indicate that the range of calculated error values is impacted by the LOGSIG transfer function in the second layer of ML_2 models and has increased compared to ML_1 models. Hence, ML_1 models have smaller error predictions than ML_2 models. ML_3 models generate more accurate results compared to all other MLP-ANN models. The ML_3 models'

results are shown in **Error! Reference source not found.** and Table 5.

Table 4: Prediction performance of the proposed ML_3 models

Number of neurons			Testing data		
Hidden layer 1 (TANSIG)	Hidden layer 2 (TANSIG)	Hidden layer 3 (TANSIG)	MAE	RMSE	MAPE(%)
3	5	7	56.656	65.273	5.016
4	3	6	22.142	28.379	1.199
5	2	7	132.284	179.348	7.472
3	7	4	25.691	31.867	1.317
5	9	6	44.378	54.096	2.244
2	4	9	42.321	48.819	2.361
8	3	5	28.116	33.294	2.588
7	7	2	38.881	51.047	1.788
6	3	4	60.932	105.214	2.113
4	4	7	42.771	47.428	1.909

Table 5: Prediction performance of the proposed ML_3 model with the structure of [4 3 6]

Day	Actual values	Predicted values
1	1411	1439
2	1634	1626
3	1972	1985
4	1512	1562
5	2102	2103
6	2311	2306
7	2456	2480
8	2521	2569

Radial Basis Function Artificial Neural Network (RBF-ANN)

Various RFB-ANNs are developed to investigate the optimal model. The collected data is divided into two groups: training data set, testing data set. 145 records of data are used to train the model, and 8 data is used to evaluate the trained model performance. It should be noted that the data for each group is selected randomly in each run. The training process of the RBF-ANN model continues until the optimum performance is obtained. The spread value of the model is set to 5, and the Gaussian function is adopted as the transfer function for the kernels. Various structures were examined based on the number of kernels. The results are presented in Table 6. Based on this table, Model 7 achieved the highest accuracy in the prediction because of the lowest MAE, RMSE, and MAPE values, among other models. High accuracy of the RBF-ANN model shows that proper values for the spread, and the number of kernels in the hidden layer have been determined in trial and error process. Also, the optimum values for the centers and weights are calculated during the training process.

Table 6: Prediction performance of the proposed RBF-ANN models

Model	Number of Kernels	Testing Data		
		MAE	RMSE	MAPE(%)
Model 5	5	50.956	56.793	3.454
Model 6	10	35.070	40.176	2.407
Model 7	12	21.319	23.459	1.227
Model 8	16	24.219	28.228	1.326
Model 9	20	28.441	32.940	2.906

Table 7 and Fig. 10 shows the performance of Model 7 for forecasting for COVID-19 cases for eight days.

Table 7: Predicted values for COVID-19 cases by Model 7 for eight days

Day	Actual values	Predicted values
1	2079	2059
2	1053	1050
3	2186	2167
4	2615	2581
5	2111	2144
6	1046	1016
7	2011	1993
8	1289	1303

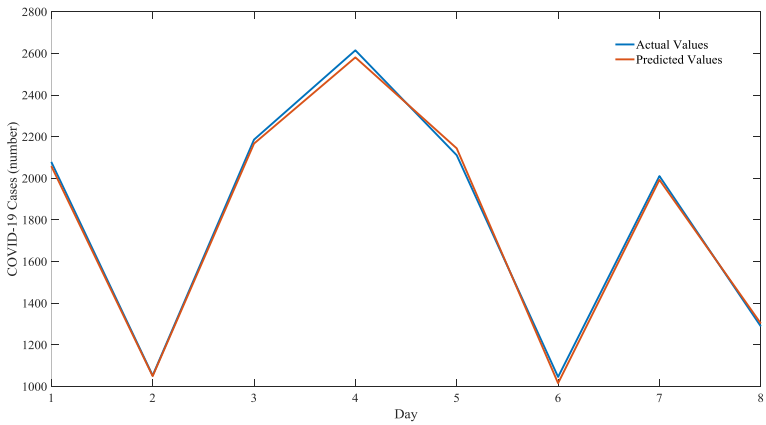

Fig. 10. Actual vs. predicted values for COVID-19 cases with Model 7 for eight days

Adaptive Neuro-fuzzy Inference System (ANFIS)

Two sets of data were used to develop the ANFIS model. One for training the model (145 records of data), and the other one for model performance evaluation (8 data). Three types of membership functions were used, including triangular membership function (trimf),

trapezoidal membership function (trapmf), and Gaussian membership function (gaussmf). The number of membership function for the first layer is set to 3. The results are presented in Table 8. Model 12 obtained the lowest MAE, RMSE, and MAPE values.

Table 8: Prediction performance of the proposed ANFIS models

Model	Membership function type	Testing Data		
		MAE	RMSE	MAPE(%)
Model 10	Trimf	56.072	69.052	3.507
Model 11	Trapmf	331.510	525.349	25.245
Model 12	Gaussmf	32.760	45.309	2.161

Table 9 and Fig.11 shows the Model 12 prediction of COVID-19 cases for eight days.

Table 9: Predicted values for COVID-19 cases by Model 12 for eight days.

Day	Actual values	Predicted values
1	1289	1184
2	1028	991
3	1030	1024
4	1529	1542
5	2445	2463
6	2262	2294
7	2316	2314
8	2621	2572

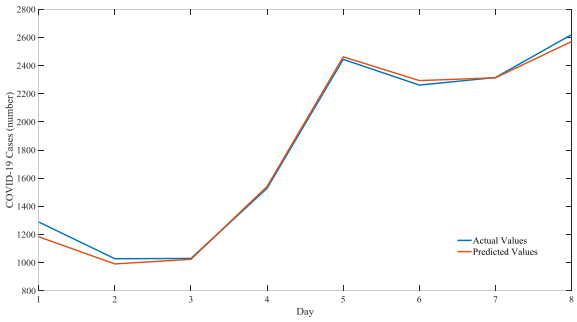

Fig.11. Actual values vs. predicted values for COVID-19 cases by Model 12 for eight days

Discussion

The overall comparison between the above three models based on error values is presented in Table 10. Model 7 can predict output values more accurately compared to other models based on MAE and RMSE values.

Table 10: Performance comparison between top developed models

Model	Type	Network Topology	Testing data		
			MAE	RMSE	MAPE(%)
1	MLP	[3-3] TANSIG, TANSIG	34.008	43.8	1.916
2	MLP	[3-4] TANSIG, LOGSIG	32.035	37.908	1.377
3	MLP	[4-3-6] TANSIG, TANSIG, TANSIG	22.142	28.379	1.199
4	MLP	[4-3-6] TANSIG, TANSIG, LOGSIG	23.578	35.555	1.045
7	RBF	[12 kernels] - Gaussian function	21.319	23.459	1.227
12	ANFIS	Three Gaussian membership function	32.76	45.309	2.161

A comprehensive comparison between models ML_1, ML_2, ML_3, ML_4, RBF-ANN, and ANFIS is presented in Table 11. This table shows the dispersion index (range, mean, and standard deviation) of calculated errors for each group of the models. According to Table 11, ML_1 models have the lowest dispersion index among MLP-ANN models, although Model 3, which belongs

to ML_3 obtained the lowest MAE and RMSE value. In overall, RBF models achieved the lowest MAE and RMSE values among other developed models.

Table 11: A comprehensive comparison between the models

Model	MAE			RMSE			MAPE(%)		
	Range	Mean	Std.	Range	Mean	Std.	Range	Mean	Std.
ML_1	25.291	45.735	8.979	33.475	56.975	11.526	3.144	2.646	1.094
ML_2	188.711	76.931	74.299	252.041	98.360	93.078	13.635	4.311	4.769
ML_3	110.142	49.417	31.699	150.969	64.477	45.969	6.273	2.801	1.953
ML_4	76.207	53.915	24.899	109.591	68.553	34.655	3.426	2.734	1.172
RBF	29.637	32.001	11.790	33.334	36.319	13.003	2.227	2.264	0.975
ANFIS	298.750	140.114	166.163	480.040	213.237	270.558	23.084	10.304	12.956

The RBF model with 12 kernels was also applied to predict COVID-19 cases for 31 days in order to investigate its performance for medium-term forecasts. The achieved MAE, RMSE, and MAPE are 34.742, 44.405, and 2.738, respectively. *Table 12* and *Fig.* **12** shows the Model 12 prediction of COVID-19 cases for 31 days.

Table 12: Predicted values for COVID-19 cases by Model 12 for 31 days

Day	Actual values	Predicted values
1	2206	2204
2	1657	1651
3	1972	1994
4	1192	1182
5	385	479
6	1997	1995
7	1806	1793
8	2586	2676
9	1787	1831
10	1168	1221
11	2886	2851
12	1209	1240
13	595	667
14	802	765
15	1683	1641
16	1294	1347
17	2180	2213
18	2901	2872
19	1762	1795
20	2667	2578
21	1574	1580
22	2621	2603
23	1411	1414
24	2456	2502
25	2566	2515
26	2392	2392

Day	Actual values	Predicted values
27	3186	3274
28	1808	1787
29	1617	1589
30	2500	2512
31	2079	2093

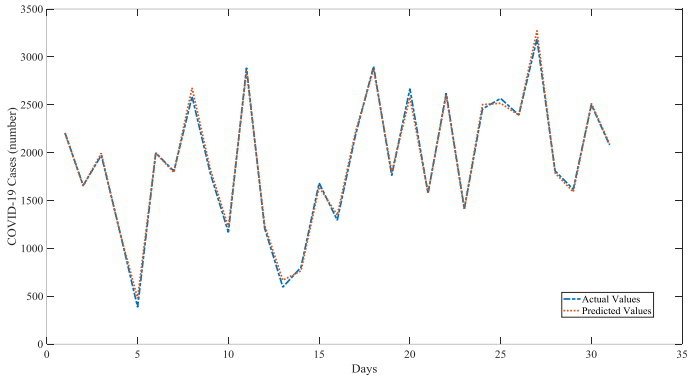

Fig. 12. Actual values vs. predicted values for COVID-19 cases by Model 12 for 31 days

CONCLUSION

The world is facing a crisis called COVID-19, which has devastating political, economic, and social consequences in all over the world. So far, countries have adopted different policies to deal with this crisis, including social distancing, teleworking, and home quarantine. Prediction methods are efficient tools that can help governments to control and manage the outbreak of COVID-19. COVID-19 cases prediction could help policymakers to make strategic decisions, including closing borders, designing supply chains for medical and health equipment, and enacting new laws.

This study proposed three types of artificial neural networks to forecast the number of COVID-19 cases based on five factors in Iran. We collected the data for 153 days. Then the collected data were divided into three groups: training data set (130 data), validation data set (15 data), and test data set (8 data). The training data set was used to train the model. The validation data set was used to determine whether the model is being trained enough for prediction or not? The test data was used to evaluate model performance. After validation of the model, the data of the last 153 days can be used to predict the COVID-19 cases in the next 8 days. Then we employed the developed RBF model with 12 kernels to predict COVID-19 cases for 31 days to examine the performance of the model in medium-term predictions. The prediction results showed that radial basis function artificial neural network models have the capability to estimate the output variable more accurately compared to other models. Various prediction models have been proposed in the literature. One of the main limitations of prediction studies is lack of access to complete historical data. On the other hand, the available data may also have errors that can mislead the forecasting process. Therefore, we suggest future researchers to consider data refinement in their studies.

ACKNOWLEDGMENT

The authors would like to express their grateful for the efforts of the editor and valuable comments of the respected reviewers.

REFERENCES

Abbas, A. K., Al-haideri, N. A., & Bashikh, A. A. (2019). Implementing artificial neural networks and support vector machines to predict lost circulation. *Egyptian Journal of Petroleum*, *28*(4), 339–347.

Acheampong, A. O., & Boateng, E. B. (2019). Modelling carbon emission intensity: Application of artificial neural network. *Journal of Cleaner Production*, *225*, 833–856.

Alakus, T. B., & Turkoglu, I. (2020). Comparison of deep learning approaches to predict COVID-19 infection. *Chaos, Solitons & Fractals*, *140*, 110120.

Al-Shawwa, M. O., & Abu-Naser, S. S. (2019). *Predicting birth weight using artificial neural network*.

Barto, A. G. (1984). Neuron-like adaptive elements that can solve difficult learning control-problems. *Behavioural Processes*, *9*(1).

Barua, S. (2021). Understanding coronanomics: The economic implications of the COVID-19 pandemic. *The Journal of Developing Areas*, *55*(3), 435–450.

Bickley, S. J., Chan, H. F., Skali, A., Stadelmann, D., & Torgler, B. (2021). How does globalization affect COVID-19 responses? *Globalization and Health*, *17*(1), 1–19.

Chen, Y., Yu, G., Long, Y., Teng, J., You, X., Liao, B.-Q., & Lin, H. (2019). Application of radial basis function artificial neural network to quantify interfacial energies related to membrane fouling in a membrane bioreactor. *Bioresource Technology*, *293*, 122103.

Emamgholizadeh, S., Moslemi, K., & Karami, G. (2014). Prediction the groundwater level of bastam plain (Iran) by artificial neural network (ANN) and adaptive neuro-fuzzy inference system (ANFIS). *Water Resources Management*, *28*(15), 5433–5446.

Guhathakurata, S., Saha, S., Kundu, S., Chakraborty, A., & Banerjee, J. S. (2022). A new approach to predict COVID-19 using artificial neural networks. In *Cyber-Physical Systems* (pp. 139–160). Elsevier.

Hartman, E. J., Keeler, J. D., & Kowalski, J. M. (1990). Layered neural networks with Gaussian hidden units as universal approximations. *Neural Computation*, *2*(2), 210–215.

Jackson, J. K. (2021). *Global economic effects of COVID-19*. Congressional Research Service.

Jang, J.-S., & Sun, C.-T. (1995). Neuro-fuzzy modeling and control. *Proceedings of the IEEE*, *83*(3), 378–406.

Kong, F. G., Li, Q., & Zhang, W. J. (1999). An artificial neural network approach to mechanism kinematic chain isomorphism identification. *Mechanism and Machine Theory*, *34*(2), 271–283.

Kouser, R. R., Manikandan, T., & Kumar, V. V. (2018). Heart disease prediction system using artificial neural network, radial basis function and case based reasoning. *Journal of Computational and Theoretical Nanoscience*, *15*(9–10), 2810–2817.

Li, Y., Wang, X., Sun, S., Ma, X., & Lu, G. (2017). Forecasting short-term subway passenger flow under special events scenarios using multiscale radial basis function networks. *Transportation Research Part C: Emerging Technologies*, *77*, 306–328.

Mirrashid, M. (2014). Earthquake magnitude prediction by adaptive neuro-fuzzy inference system (ANFIS) based on fuzzy C-means algorithm. *Natural Hazards*, *74*(3), 1577–1593.

Mitchell, T. M., & Mitchell, T. M. (1997). *Machine learning* (Vol. 1, Issue 9). McGraw-hill New York.

Mohandes, M., Rehman, S., & Rahman, S. M. (2011). Estimation of wind speed profile using adaptive neuro-fuzzy inference system (ANFIS). *Applied Energy*, *88*(11), 4024–4032.

Nayak, P. C., Sudheer, K. P., Rangan, D. M., & Ramasastri, K. S. (2004). A neuro-fuzzy

computing technique for modeling hydrological time series. *Journal of Hydrology*, *291*(1–2), 52–66.

Sadek, R. M., Mohammed, S. A., Abunbehan, A. R. K., Ghattas, A. K. H. A., Badawi, M. R., Mortaja, M. N., Abu-Nasser, B. S., & Abu-Naser, S. S. (2019). *Parkinson's disease prediction using artificial neural network*.

Takagi, T., & Sugeno, M. (1983). Derivation of fuzzy control rules from human operator's control actions. *IFAC Proceedings Volumes*, *16*(13), 55–60.

Tatar, A., Nasery, S., Bahadori, A., Bahadori, M., Najafi-Marghmaleki, A., & Barati-Harooni, A. (2016). Implementing radial basis function neural network for prediction of surfactant retention in petroleum production and processing industries. *Petroleum Science and Technology*, *34*(11–12), 992–999.

APPENDIX

A.1. The complete data set.

Sample number	Daily Cases	Gasoline Consumption (Million Liter)	Internet Pressure	Registered Wedding ceremony	Online transaction (Thousand Billion Rials)	Mask consumption
1	385	24	14.052	919	3.8	978624
2	523	22	13.569	971	3.9	976754
3	835	39	11.597	1039	3.2	890051
4	586	22	14.731	816	3.7	832480
5	591	29	13.09	1838	4.1	915823
6	1234	50	11.597	2236	3.3	872553
7	1076	44	13.103	1415	3	922186
8	743	25	12.279	2110	3.7	901008
9	595	31	13.645	1371	3.8	869960
10	881	36	11.086	2077	3.1	853555
11	958	44	12.945	2560	3.7	788591
12	1075	41	13.414	3285	3.5	774899
13	1289	59	10.452	1502	2.6	860722
14	1635	68	11.21	2226	2.8	759036
15	1209	40	10.31	1892	3	735410
16	1053	44	12.172	3252	3.5	817616
17	1178	44	11.983	3292	3.1	869861
18	1192	54	12.528	3031	3.1	891523
19	1046	44	11.362	2557	3.1	839534
20	1237	47	12.434	2715	3.4	767425
21	966	41	12.186	2356	3	906336
22	1028	34	12.866	1743	2.9	889564
23	1411	59	9.355	3861	3.1	810205
24	1762	64	9.917	3551	2.9	879845
25	2206	72	9.266	5239	1.7	725463
26	2389	91	7.297	3277	1.5	670035
27	2926	101	7.097	4602	1.1	601451
28	3076	103	3.652	8850	1	637187
29	2901	100	6.052	6239	1.6	587066
30	3186	129	4.145	5617	1.2	579748
31	3110	134	5.386	5579	1.2	726554

Sample number	Daily Cases	Gasoline Consumption (Million Liter)	Internet Pressure	Registered Wedding ceremony	Online transaction (Thousand Billion Rials)	Mask consumption
32	2988	106	3.621	4022	1.6	693702
33	2875	90	6.466	3564	1.5	717989
34	2715	102	4.997	5639	1.2	604614
35	2560	87	6.155	5599	1.7	726092
36	2483	92	7.876	7511	1.9	609574
37	2274	95	7.59	4813	2.4	616956
38	2089	79	6.61	4778	2.2	792618
39	1997	70	8.638	2778	2	724110
40	1634	59	9.852	2787	2.9	861000
41	1972	79	8.459	3894	2.4	719344
42	1837	66	8.566	5119	2.1	707733
43	1657	68	11.21	3238	3.1	762607
44	1617	60	9.752	2248	2.4	784497
45	1574	59	11.793	2138	2.8	661180
46	1512	60	9.159	2612	3.2	706004
47	1606	58	10.231	3277	2.9	777400
48	1499	58	9.838	3161	2.4	707908
49	1374	62	10.855	2275	3.3	792613
50	1343	56	10.041	2288	3	850183
51	1294	47	11.1	3836	2.6	824769
52	1297	59	11.938	2538	2.8	878569
53	1194	46	12.293	2378	3.4	776635
54	1030	42	12	1929	3.4	792467
55	1168	42	10.545	3088	3.3	787380
56	1134	45	11.828	1375	3.2	800198
57	1153	39	12.99	2181	2.9	860571
58	991	38	12.138	1295	2.9	895536
59	1112	42	12.483	2669	2.9	837814
60	1073	40	13.376	1310	3	760245
61	983	43	10.721	2220	3.3	779028
62	1006	41	13.51	1425	3.1	885574
63	802	34	13.941	1762	3.8	955256
64	976	36	11.245	1392	3.7	818127
65	1223	43	9.831	3673	2.9	718648
66	1323	51	10.783	3820	3.3	812852
67	1680	62	8.728	4062	2.5	833713
68	1485	60	8.879	2791	3.1	665907
69	1556	68	10.052	3734	2.5	746807
70	1529	54	9.072	3783	2.4	778592
71	1383	49	11.931	4149	2.9	898917
72	1683	57	11.369	4877	2.8	843317
73	1481	67	10.866	1662	3	930093
74	1958	81	10.338	2466	2	813905
75	1808	75	8.152	4150	2.5	816576
76	2102	82	8.907	5509	2.4	710877

Sample number	Daily Cases	Gasoline Consumption (Million Liter)	Internet Pressure	Registered Wedding ceremony	Online transaction (Thousand Billion Rials)	Mask consumption
77	1757	66	10.483	2187	2.2	712400
78	1806	66	10.503	4618	2.2	812988
79	2294	79	6.183	4958	2.3	599036
80	2111	80	7.134	5872	2.4	745888
81	2346	94	5.776	6453	1.8	719373
82	2392	83	6.431	5182	2.3	678437
83	2311	83	7.676	6565	2.2	673979
84	1869	73	8.283	3148	2.1	815995
85	2180	76	9.659	5753	2.6	739083
86	2023	66	10.176	2483	2.5	693094
87	1787	74	10.962	2324	2.1	756194
88	2080	77	9.469	4369	1.8	765771
89	2258	88	7.745	2534	2.1	661209
90	2819	114	6.99	7986	1.3	684776
91	2282	78	8.183	5307	2.3	815252
92	2516	101	7.659	3987	2.3	748668
93	2979	117	3.928	8143	1	707296
94	3117	121	4.645	3793	0.8	593197
95	3134	122	4.717	6321	1.4	583736
96	3574	116	4.914	10332	1.1	653976
97	2886	98	3.897	7869	1.7	655302
98	2269	86	7.748	3728	2.3	657396
99	2364	90	7.259	5086	1.6	648941
100	2043	70	8.2	4071	2	654028
101	2095	69	8.31	4302	2.6	771077
102	2011	81	7.121	3951	2.1	839369
103	2218	93	7.021	3058	1.9	739478
104	2389	86	6.417	6942	1.9	816692
105	2410	91	6.5	4153	2.3	659424
106	2472	107	6.448	2596	2.3	781274
107	2449	90	6.572	4953	2	570758
108	2563	98	5.921	6314	1.4	580332
109	2612	80	4.8	3737	1.4	739571
110	2586	83	7.414	4429	1.5	679052
111	2615	96	4.783	6411	1.7	673923
112	2322	89	8.172	3860	1.7	666682
113	2368	97	8.441	7144	2.4	696897
114	2573	101	5.097	7221	1.8	675254
115	2445	91	7.983	5087	2.3	705972
116	2531	88	6.631	3626	1.9	611127
117	2595	96	5.107	7022	2	597819
118	2628	89	6.672	3699	1.3	730038
119	2456	79	6.779	4384	2.3	590341
120	2489	83	6.383	6542	2	611161
121	2536	94	5.241	6041	1.7	802132

Sample number	Daily Cases	Gasoline Consumption (Million Liter)	Internet Pressure	Registered Wedding ceremony	Online transaction (Thousand Billion Rials)	Mask consumption
122	2457	104	7.99	7144	1.7	754901
123	2549	85	7.283	5072	1.4	692101
124	2652	91	5.259	7332	2.1	726129
125	2566	99	7.99	5107	2.1	736131
126	2449	85	7.231	5356	2	593982
127	2560	90	5.886	4630	2.2	753994
128	2613	99	5.476	4715	1.3	645187
129	2637	92	6.7	5213	1.4	599529
130	2691	100	6.383	8114	1.6	628552
131	2079	80	7.183	4406	2.2	832639
132	2262	81	6.614	5376	2.5	804071
133	2397	87	8.103	6042	2.3	741120
134	2186	87	6.869	4270	2.2	742417
135	2349	90	6.355	4872	2.5	712913
136	2521	101	8.172	2871	1.9	596487
137	2388	93	8.817	2609	1.6	684646
138	2500	99	6.152	5738	1.6	709774
139	2379	94	9.038	4433	2.3	770811
140	2166	80	8.986	3780	2.5	673660
141	2182	85	7.793	6125	2.5	632136
142	2414	80	7.403	3790	2.1	676219
143	2625	91	5.024	6849	1.5	583350
144	2586	91	7.207	5508	1.6	683234
145	2621	107	5.552	7856	1.4	689998
146	2489	89	7.238	7033	1.9	771075
147	2316	73	8.731	6924	2.5	653554
148	2333	94	8.114	6566	1.7	681997
149	2434	87	5.497	4546	2	633872
150	2667	90	6.472	7966	2	646571
151	2636	96	6.838	7236	2	761530
152	2621	91	5.79	4039	1.4	754814
153	2674	103	7.841	7533	1.7	638741